



FLUCOME 2009

10th International Conference on Fluid Control, Measurements, and Visualization
August 17–21, 2009, Moscow, Russia

AN EXPERIMENTAL OBSERVATION OF 3-D SCRAMJET INLET FLOW IN SHOCK TUNNEL

Bo Huang, Zhufei Li, Jiming Yang, Xisheng Luo

ABSTRACT

An experimental study was carried out on three-dimensional scramjet inlet flow. Six 3-D inlet models with different swept and wedge angles were examined in a M4.5 shock tunnel by means of oil-film visualization technology and high speed schlieren photography. As a valuable supplement, 2-D numerical simulations were also conducted. The schlieren photos clearly show the very complex flow structure in the inlet, which is mainly caused by the shock wave-boundary interaction. The shock wave interaction consists of shock waves and viscous separation regions. These phenomena are also confirmed by the numerical simulations. The oil-film photos capture the flow patterns near the walls of the inlet. The fin shock, the separation line and the attachment line can be identified. It seems that interactions of shock wave caused by the cowl with the boundary layer over the top and with the boundary layer over the wedge sidewall are main flow structures, which deteriorate the flow field in the inlet.

Keywords: shockwave-boundary interaction, scramjet, hypersonic inlet, flow visualization

INTRODUCTION

As an important part of a scramjet engine, the flow quality in the inlet is one of the main factors that determine the performance of the engine. Shockwave-boundary layer interaction (SWBLI or SBLI) may cause strong harmful flow such as separation in the inlet, which can deteriorate the flow field and reduce the efficiency significantly. Many gas dynamic phenomena arising in the flow around hypersonic inlets remain unknown because of their complexity, and the explanation probably still comes from the first-hand experimental observations.

Numerous related investigations, such as swept-shock/boundary layer interactions in three-dimensional configurations, have been carried on for several decades. There are several models of the flow field of SWBLI caused by swept shockwave and boundary layer over plate. In this case, the interactions occur between two intersecting surfaces, and the separation bubble is actually a conical flat vortex on both surfaces [1]. Other important cases of the SWBLI include the interaction caused by an impinging shockwave with a boundary layer over a plate, and the separation occurring in corner in supersonic flow which will cause an originating shock wave [2]. Both of these have been studied extensively ([3]~[5]). But most of these researches used a simple experimental model. In a real supersonic inlet, flow structure, especially the interaction of shockwaves and boundary layer, is far more complex. In our experiments, models are designed as smaller copies of the real three-dimensional scramjet inlet. Oil-film technology and schlieren photograph with high speed CCD camera are employed to visualize the

flow field in the model. With numerical simulations, we can analyze the structure of flow field in the three-dimensional supersonic inlet. Shock wave structure and their interactions with boundary layer can be identified, which also demonstrates a significant non-uniformity and three dimensional characteristics.

DESCRIPTION OF EXPERIMENTS

The experiments were performed in the JB-430 shock tunnel in the Shock Wave Laboratory in University of Science and Technology of China, which is a straight-through-type shock tunnel. The experimental facility, as shown in Fig.1, consists of a nozzle of 1.35m long, a test section with an area of $50 \times 50 \times 100$ cm, and a shock tube with an inner diameter of 106 mm that has a high pressure section (HPS) of 3.8 m and a low pressure section (LPS) of 12.65 m. Two diaphragms are employed: a prescribed alumina plate as the main diaphragm separating the HPS and LPS, and a plastic sheet as the second diaphragm isolating the LPS from the vacuum tank and the nozzle. The vacuum tank and the nozzle are evacuated to prior to experiment, and the LPS is filled with 0.6 bar of air. The HPS is filled with a mixture of air and helium from the gas bottles. All experiments in this study were carried out at a Mach number of 4.5, a stagnation temperature of 1100K, and a unit Reynolds number of 2×10^6 /m. Typical run time is 10 milliseconds. A high speed CCD camera working at 1000fbps is adopted to get 6~8 schlieren photographs of the flow field can be obtained in each run.

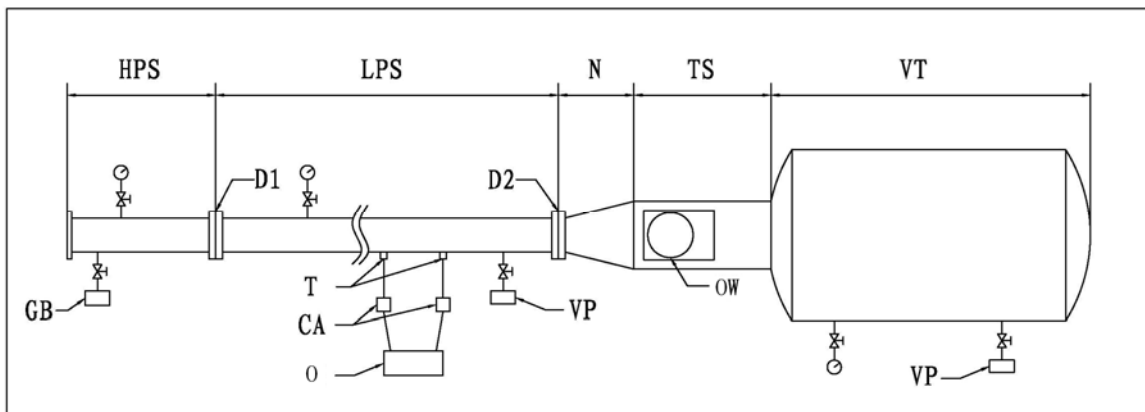


Fig.1. Schematic of the shock tunnel. HPS: high pressure section, LPS: low pressure section, N: nozzle, TS: test section, VT: vacuum tank, GB: gas bottle, T: transducer, CA: charge amplifier, D1: main diaphragm, D2: second diaphragm, VP: vacuum pump, OW: optical window, O: oscilloscope

Six models were used in the experiments. To know details of the flow in the inlet by optic technology directly, parts of the surface of the model are replaced by optical windows, and schlieren photography is used to visualize the flow field. Fig.2 sketches the geometry of the model and Fig.3 is the photograph of two of the models. Detail of models are listed in Table.1. Model 1, 3 and 5 are used to take photos from side-view, and Model 2, 4 and 6 are used to take photos from top-view.

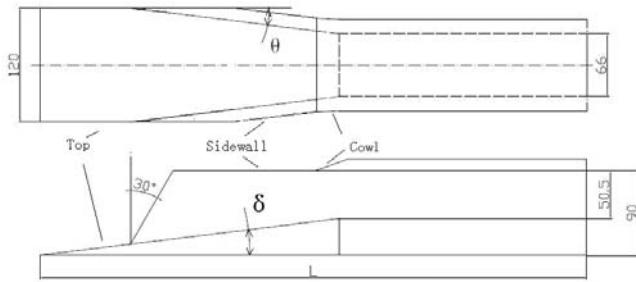


Fig. 2. Geometry of the model (dimensions are in mm)



Fig.3. Photo of two models with optical windows

Table 1. Detail of models

No.	1	2	3	4	5	6
δ	7°	7°	9°	9°	11°	11°
θ	7°	7°	9°	9°	11°	11°
L (mm)	574	574	503	503	458	458
Location of glass	Sidewalls	Top & Cowl	Sidewalls	Top & Cowl	Sidewalls	Top & Cowl

Details of the area near the surface are also necessary to investigate the flow structure in the inlet since the irregular geometry of the model makes the schlieren photography difficult to apply at the front part of the inlet. Oil-film is an effective visualization technology to demonstrate the flow configuration close to the wall surface. We applied a mixture of methyl silicone oil and titanium dioxide, and set the mixture on the surface as points at diameter of 1~2mm, which is an effective method used in the shock tunnel [6].

NUMERICAL METHOD

The numerical method VAS2D [7] is employed to simulate the simplified version of the inlet model. The finite-volume method is used to discretize the two-dimensional Navier-Stokes equations by directly applying them to each non-overlapping control volume. The MUSCL-Hancock scheme [8], a second-order upwind scheme, is adopted to compute the flux through the cell interface. In this method, the equations are discretized on an unstructured quadrilateral mesh that adapts to the time-dependent flow. The adaptation criterion utilizes the maximum of the error sensors of the density and the two velocity components.

The computational geometry uses a scaled down model, 10% of the actual experimental model. An adaptation level of 4 is used. Grid number is in the range of $1 \times 10^5 \sim 1.5 \times 10^5$. In the numerical simulation, we used the boundary mesh in the region close to the surface. There are ten rows of mesh in the boundary layer. Size of the row most close to the surface is 0.08 mm. Growth factor is 1.2 and the largest boundary layer mesh has a size of 0.5 mm.

RESULTS

According to the results of related investigation, there are three main regions of interaction in our three-dimensional supersonic inlet. They are I) shock wave caused by the wedge sidewalls and the boundary layer over the top of the inlet (Type I for short), II) shock wave caused by the cowl and the boundary layer over the top (Type II) and III) shock wave caused by the cowl and the boundary layer over the wedge sidewall (Type III). In this observation, suitable visualization technology was employed for different type of the interactions.

Fig.4 shows typical schlieren photos for models with a wedge angle of 7° together with the numerical results. The upper two figures from the simulation represent the wave structures from the side-view and top-view. In these two models, the leading oblique shock locates in front of the cowl. Therefore, in the side-view schlieren photo, only the oblique shock from the cowl and its reflection are presented, see the middle-left photo of Fig.4. The two oblique shocks from the side-walls interact with the Prandtl-Meyer (P-M) expansion waves can be seen in the top-view photo, as shown in the right side of Fig.4. The lower two figures of Fig.4 are the numerical counterparts of the experimental schlieren photos. Type II SWBLI can be clearly observed in both simulations and experiments. Actually for the wedge of the sidewall and the top, it's almost impossible to take photo of the flow field of the front of inlet. Therefore, all schlieren photos show the rearward of the inlet and Type I interaction region couldn't be seen by the schlieren.

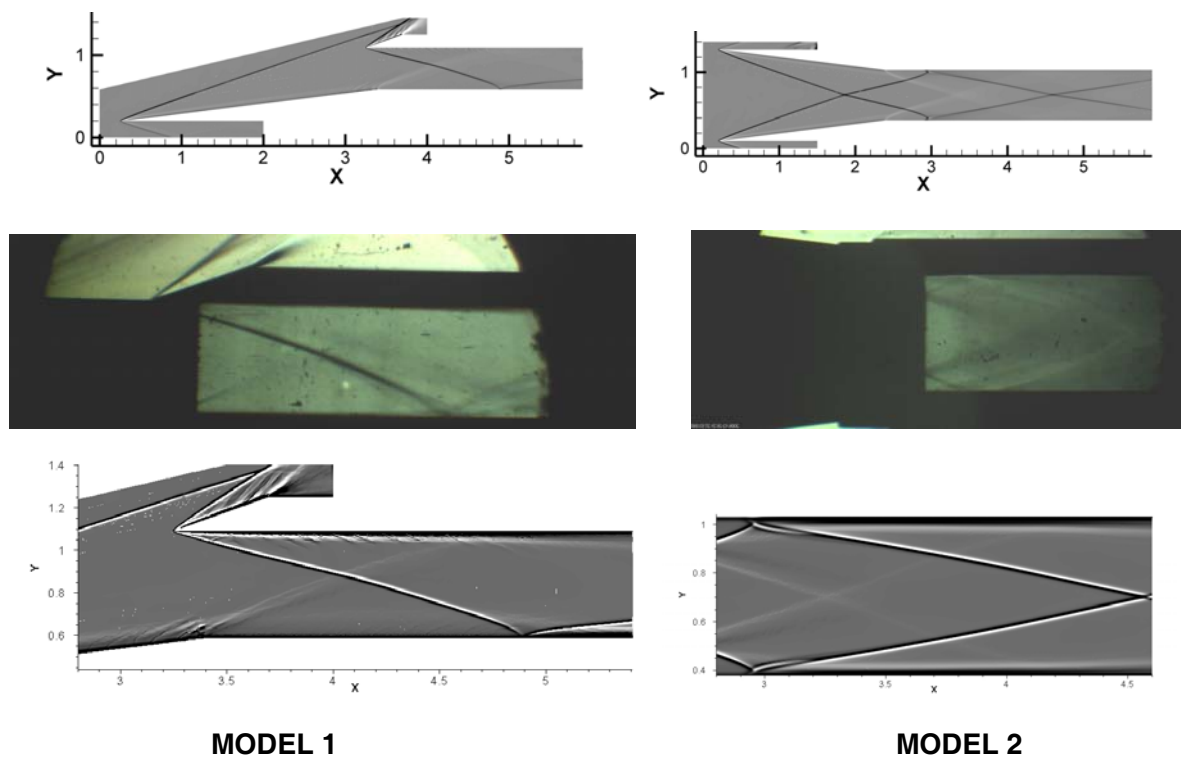
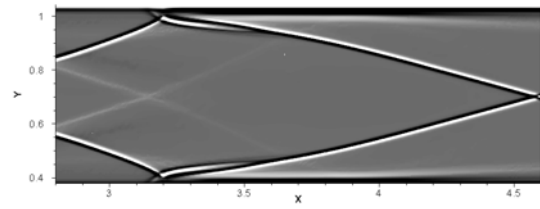
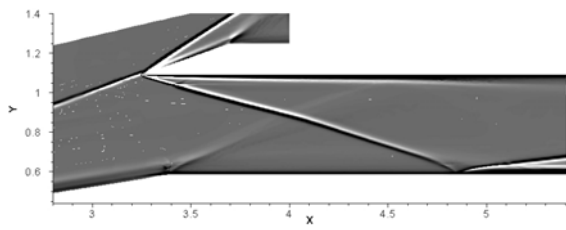
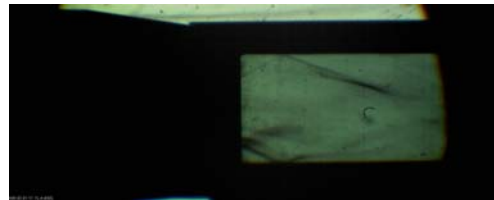
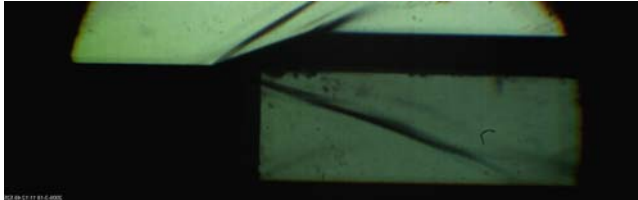
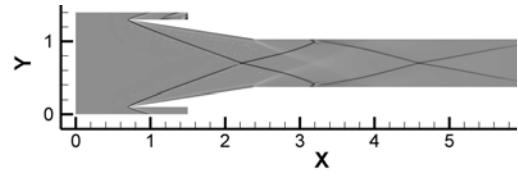
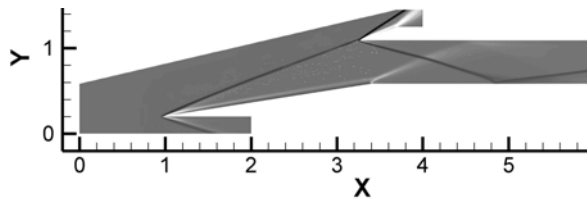


Fig.4. Results for model 1 and 2

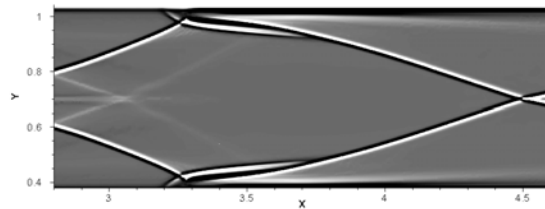
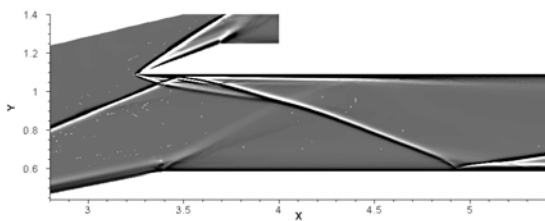
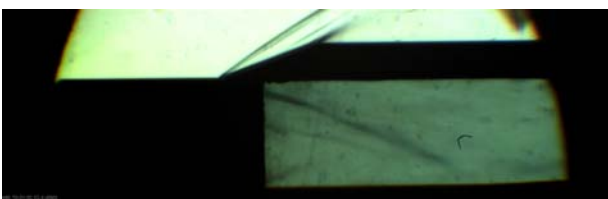
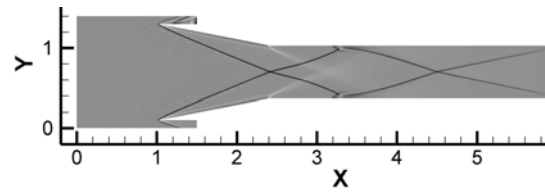
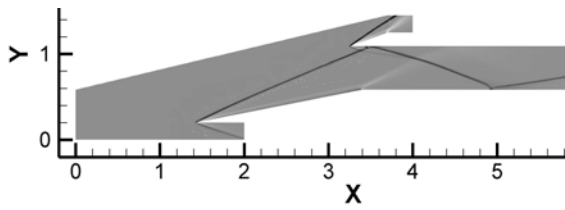
Typical schlieren photos for models with a wedge angle of 9° are shown in Fig.5, together with the corresponding numerical results. In these two models, the leading oblique shock is very close to the cowl but still away from the inner part. Therefore, the wave structure is almost the same as that in Fig.4. Type II SWBLI can be clearly observed in both simulations and experiments too.



MODEL 3

MODEL 4

Fig.5. Results for model 3 and 4



MODEL 5

MODEL 6

Fig.6. Results for model 5 and 6

Increasing the wedge angle further will cause the leading shock wave moving further downstream of the cowl. Fig.6 shows typical schlieren photos for models with a wedge angle of 11° together with the numerical results. In these two models, the leading oblique shock locates and reflects behind the cowl. In the middle-left figure of Fig.6, two shocks are presented too. One is the reflection of the leading shock and the other is the oblique shock from the cowl. The numerical schlieren picture (the lower-left figure of Fig.6) shows a similar wave structure of two shock waves. The two oblique shocks from the side-walls interact with the P-M expansion waves can be seen in the top-view photo, as shown in the right side of Fig.6. In the lower-right figure, a slip stream is shown, which couldn't be identified in the schlieren photo. This is because the sensitivity of the schlieren is not enough to capture this structure.

Optical technology combining 2-D numerical simulation can obtain the information of dimensional structure of the flow field. But it's difficult to show the detail of the flow field close to the surface. For example, Type I interaction region is hard to be investigation by this technology in this observation. With the oil-film technology, flow field close to the surface can be visualized. Fig. 7 shows the result of the oil-film visualization, from which the Type I, II & III regions of separation can be obtained.

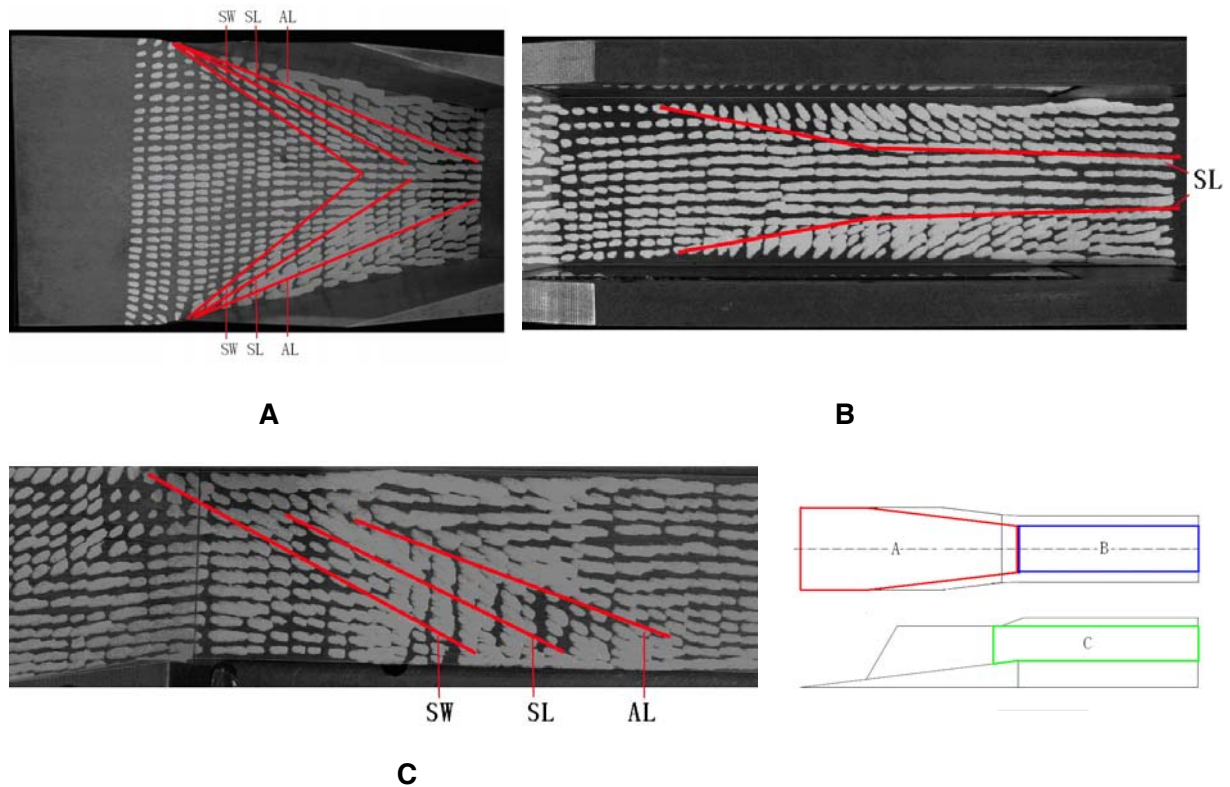


Fig.7. Photographs of oil-film in three parts of model 5.

Three parts of the model 5 are used for oil-film visualization, i.e. the top-front, the top-rear and the side wall. Fig.7(A) shows Type I interaction region occurring at the top-front wall. The inviscid fin shockwave (SW), separation line (SL) and attachment line (AL) are represented with lines. According to Garrison's results [5], there is a triple-shock interaction at the part of inlet in Fig.7(A). A half-conical region of separation at the corner of two intersecting surfaces can be shown by the movements of the oil points there. In Fig.7(B), region of separation on top-rear wall is shown as Type II of interaction which is caused by the cowl-shockwave and the boundary layer on the top. For the corner of the sidewall and the

top, there is a pressure gradient close to the surface of the top which across the inlet from the sidewall to the central of the inlet. As a result, the separation region shows a conical flat vortex. Separation lines are marked too. On the sidewall as shown in Fig.7(C), we can see the shock wave caused by the cowl and Type III interaction region. Cowl-shockwave, separation line, attachment line and region of separation on the sidewall are shown in the photo. From Fig.7(B) and Fig.7(C), it seems that Type II and III of interactions are main flow structures which deteriorate the flow field in the inlet. It is also found that shockwave caused by the cowl plays an important role of these interactions.

There are two important factors which affect the SWBLI. One is the strength of shockwave and the other is the property of boundary layer such as the thickness δ , the Reynolds number, etc. In the downstream of the inlet, δ is bigger than that in the upstream. Therefore, the separation region in Fig.7 (B) is larger than that in Fig.7 (A). So is the separation region in Fig.7(C). Interactions in Type I and Type III cause significant non-uniformity and three dimensional characteristics in the inlet. How to reduce these separations by boundary layer control methods is a crucial problem. Pumping at the area where shockwave impinges on the top and sidewalls maybe effective because it will reduce the thickness of the boundary layer.

CONCLUSION

In this observation, six three-dimensional scramjet inlet models are examined in the shock tunnel with oil-film technology and high speed schlieren technology. Flow structures including interaction regions (such as shock waves and viscous separation regions) are presented and compared with the results of the numerical simulation. With different swept and wedge angles, leading shockwaves are at different location. Especially in the model with a wedge angle of 11° , shockwave structure is very different from other models with wedge angle of 7° and 9° . Oblique shock from the cowl interacts with the boundary layer on the top and the sidewalls where separation region could be shown clearly. These separation regions deteriorate the flow field in the inlet. To demonstrate the effect of pumping to reduce the separation, additional experiments are required. On the other hand, three-dimensional numerical simulation becomes necessary in order to know the details of the flow field that is beyond the current experimental method.

REFERENCES

- [1].A.G. Panaras (1996) Review of the physics of swept-shock/boundary layer interactions. Prog. Aerospace Sci., 32:173-244.
- [2].W. H. Heiser, D. T. Pratt (1994) Hypersonic Airbreathing Propulsion. AIAA Education Series
- [3].Y.P. Goonko, A.F. Latypov, I.I. Mazhul, A.M. Kharitonov, M.I. Yaroslavtsev, P. Rostand (2003) Structure of flow over a hypersonic inlet with side compression wedges. AIAA JOURNAL, 41 (3): 436-447.
- [4]. T. Neuenhahn, H. Olivier (2006) Influence of the wall temperature and the entropy layer effects on double wedge shock boundary layer interactions. AIAA Paper 2006-8136
- [5].T.J. Garrison, G.S. Settles, et al. (1996). Measurements of the triple shock wave turbulent boundary-layer interaction. AIAA Journal 34(1): 57-64
- [6]. Shifen Wang, Yu Wang, Peng Liu(1993) Surface feature in hypersonic swept shock and boundary layer interaction. Acta Aeronautica et Astronautica Sinica 14(9): 449-454.
- [7]. M. Sun, K. Takayama (1999) Conservative smoothing on an adaptive quadrilateral grid. J. Comp. Phys. 150:143–180.
- [8]. B. van Leer (1984) On the relation between the upstream-differencing schemes of Godunov, Engquist–Osher and Roe. SIAM J. Sci. Statist. Comput. 5:1–20.